

Analysis and Design of Passive Polyphase Filters

Jouni Kaukovouri, *Student Member, IEEE*, Kari Stadius, *Member, IEEE*, Jussi Ryyänen, *Member, IEEE*, and Kari A. I. Halonen, *Member, IEEE*

Abstract—Passive RC polyphase filters (PPF) are analyzed in details in this paper. First, a method to calculate the output signals of an n -stage PPF is presented. As a result, all relevant properties of PPFs, such as amplitude and phase imbalance, and loss, are calculated. The rules for optimal pole frequency planning to maximize the image-reject ratio provided by a PPF are given. The loss of PPF is divided into two factors, namely the intrinsic loss caused by the PPF itself and the loss caused by termination impedances. Termination impedances known a priori can be used to derive such component values, which minimize the overall loss. The effect of parasitic capacitance and component value deviation are analyzed and discussed. The method of feeding the input signal to the first PPF stage affects the mechanisms of the whole PPF. As a result, two slightly different PPF topologies can be distinguished, and they are separately analyzed and compared throughout this paper. A design example is given to demonstrate the developed design procedure.

Index Terms—Image reject, loss, passive polyphase filter, quadrature generation, transceivers.

I. INTRODUCTION

Quadrature signal generation is an essential part of modern telecommunication RF front-end signal processing. Nowadays commonly used direct-conversion and low-IF receivers, see e.g. [1-3], require two local oscillator (LO) signals in quadrature. Three commonly applied methods for in-phase (I) and quadrature-phase (Q) signal generation are the use of phase shifter, divide-by-two circuit, and coupled oscillator, see e.g. [4]. It's a manifold matter to select among these. All are relevant and selection depends on targeted system, selected radio architecture, and applied IC process. Amplitude and phase balance of the generated I and Q signals affect strongly on the image rejection of the receiver and thus on the quality of reception.

Sequence asymmetric polyphase RC networks [5] are

Manuscript received February 28, 2007; revised September 3, 2007. This work was supported in part by the Nokia Research Center, the Nokia Foundation, and the Finnish Funding Agency for Technology and Innovation.

J. Kaukovouri, K. Stadius, J. Ryyänen, and Kari A. I. Halonen are with the Electronic Circuit Design Laboratory/SMARAD2, Helsinki University of Technology, FIN-02015 Espoo, Finland (phone: +358-9-451-2988; fax: +358-9-451-2269; e-mail: jkaukovu@ecdl.hut.fi).

Copyright (c) 2007 IEEE. Personal use of this material is permitted. However, permission to use this material for any other purposes must be obtained from the IEEE by sending an email to pubs-permission@ieee.org.

commonly used for I/Q generation, and also for IF-signal phase shifting and summing in analog-IF domain [1]. Somewhat surprisingly, despite of their vast popularity in RF IC implementations, detailed analyses in open forums remain limited [6-16] and explicit formulas given do not cover all relevant issues. The aim of this paper is to thoroughly analyze the characteristics of an n -stage polyphase RC network, and based on this analysis we will present design guidelines for optimum configuration and dimensioning. Since the motivation for this work originates from practical RF IC development, we will also consider the impact of device tolerances and the effect of parasitic capacitance, thus keeping in mind realization limits of actual monolithic capacitors and resistors.

The paper is occupied with some intense mathematical analysis, and therefore we will here briefly introduce the content for guiding the reader. The analysis presented in this paper is mainly focused to PPFs with maximum of three stages, because the PPFs implemented on IC seldom have more stages. The equations can be derived for higher order PPFs too with the methods presented in this paper. Section II describes the basic structure of a passive RC polyphase filter and introduces two types of signal feeding techniques. According to input configuration we call the variants Type I and Type II PPF. These are depicted in Figures 1 and 2. Since this slight change on input feeding has significant impact on the PPF performance, we carry out the analysis of both variants throughout the text. The transfer functions, and consequently frequency response, and gain and amplitude imbalance, are also derived here. Section III focuses on image rejection and bandwidth issues, and Section IV is devoted to intrinsic loss analysis. The impact of input and output impedance and port termination are covered in Section V. Since device's parasitic capacitance and deviation from nominal value are inherent to any actual IC implementation, these are studied in Sections VI and VII, respectively. In Section VIII we summarize the results of mathematical analysis in plain words and provide design guidelines together with a design example.

II. INTRODUCTION TO THE ANALYSIS OF POLYPHASE FILTERS

The analysis of polyphase filters is started by calculating the output signals and the frequency responses of a single PPF stage. An n^{th} stage of a polyphase filter is shown in Fig. 3a.

CAS-I 5126 Kaukovouri

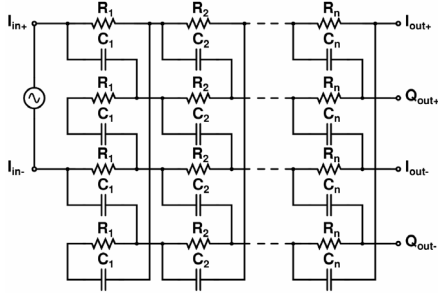


Fig. 1. Type I polyphase filter.

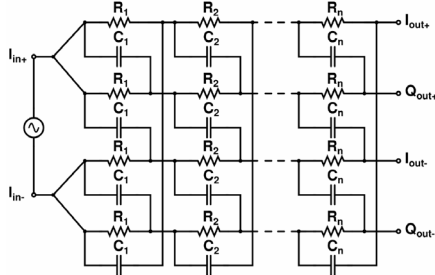


Fig. 2. Type II polyphase filter.

The output is loaded with impedance Z_{L_n} representing the input impedance of the following stage. This can be a next PPF stage, a mixer switch, or an amplifier input. When a balanced input signal is applied to I input, the Q input nodes are virtual grounds whatever the source impedance is, and vice versa. This is proven in Appendix A. When the load is the next PPF stage, the load impedance Z_{L_n} is presented with an equivalent circuit shown in Fig. 3b. The output voltages of n^{th} PPF stage shown in Fig. 3a can be calculated by voltage division and superposition rules. For example, the output node voltage $I_{out+,n}$ is calculated as follows

$$V_{I_{out+,n}} = V_{I_{in+,n}} \frac{(sC_n)^{-1} \parallel Z_{L_n}}{R_n + (sC_n)^{-1} \parallel Z_{L_n}} + V_{Q_{in-,n}} \frac{R_n \parallel Z_{L_n}}{(sC_n)^{-1} + R_n \parallel Z_{L_n}}. \quad (1)$$

The first right-hand side term is achieved by applying the voltage signal to the input node $I_{in+,n}$ and grounding all the other inputs. Thus, the capacitor C_n connected to the input node $Q_{in-,n}$ is in parallel with the load impedance Z_{L_n} of the output node $I_{out+,n}$. The resulting output signal is calculated with voltage division. The other output voltages can be calculated similarly. In a general case, when each output node is loaded with impedance Z_{L_n} , the differential I- and Q-output signals are

$$\Delta V_{I_{out,n}} = \frac{Z_{L_n}}{R_n + Z_{L_n} + sR_n C_n Z_{L_n}} (\Delta V_{I_{in,n}} - sC_n R_n \Delta V_{Q_{in,n}}), \quad (2)$$

$$\Delta V_{Q_{out,n}} = \frac{Z_{L_n}}{R_n + Z_{L_n} + sR_n C_n Z_{L_n}} (sC_n R_n \Delta V_{I_{in,n}} + \Delta V_{Q_{in,n}}), \quad (3)$$

respectively. Equations (2) and (3) are then represented in an useful matrix notation

$$\begin{bmatrix} \Delta V_{I_{out,n}} \\ \Delta V_{Q_{out,n}} \end{bmatrix} = \frac{Z_{L_n}}{R_n + Z_{L_n} + sC_n R_n Z_{L_n}} \begin{bmatrix} 1 & -sC_n R_n \\ sC_n R_n & 1 \end{bmatrix} \begin{bmatrix} \Delta V_{I_{in,n}} \\ \Delta V_{Q_{in,n}} \end{bmatrix}. \quad (4)$$

When the n^{th} PPF stage is followed by a next PPF stage, the

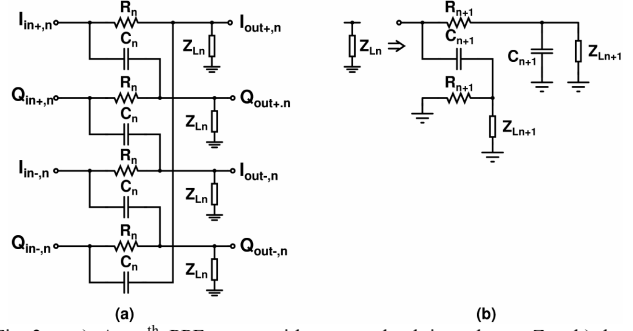


Fig. 3. a) An n^{th} PPF stage with output load impedance Z_{L_n} , b) load impedance of n^{th} PPF stage, when the load is a next PPF stage. $Z_{L_{n+1}}$ represents the loading of the $n+1^{\text{th}}$ stage.

input impedance of stage $n+1$ acts as the load Z_{L_n} . From Fig. 3b the equivalent load impedance Z_{L_n} for stage n can be calculated as

$$Z_{L_n} = \frac{R_{n+1} + Z_{L_{n+1}} + sC_{n+1} R_{n+1} Z_{L_{n+1}}}{1 + sC_{n+1} (R_{n+1} + 2Z_{L_{n+1}})}. \quad (5)$$

R_{n+1} , C_{n+1} , and $Z_{L_{n+1}}$ are the resistor values, capacitor values, and the load impedance of the $n+1^{\text{th}}$ stage, respectively.

A. About PPF Topologies, Terminology, and Notation

The manner of feeding the input signal to the first stage affects the operation of the PPF. In the case shown in Fig. 1, the Q-inputs of the first stage are signal grounds, i.e. $\Delta V_{Q_{in,1}} = 0$. In Fig. 2 the input signal is injected in a dual-feed manner, i.e. $\Delta V_{Q_{in,1}} = \Delta V_{I_{in,1}}$. For the rest of this paper, the former topology is called as Type I PPF and the latter topology is Type II PPF. In following equations, the upper index I or II is used to indicate the type of the PPF.

B. PPF Frequency Responses and Balances

The output voltages of an n -stage PPF can be calculated by multiplying the matrix (4) of each PPF stage, and by using (5) when taking into account the effect of load of the next stage. At first, differential output voltages of a single-stage PPF Type I are calculated as

$$\Delta V_{I_{out}}^I(s) = \frac{Z_{L1}}{R_1 + Z_{L1} + sR_1 C_1 Z_{L1}} \Delta V_{I_{in}}^I(s), \quad (6)$$

$$\Delta V_{Q_{out}}^I(s) = \frac{sR_1 C_1 Z_{L1}}{R_1 + Z_{L1} + sR_1 C_1 Z_{L1}} \Delta V_{I_{in}}^I(s). \quad (7)$$

The ratio between I and Q output signals is

$$\frac{\Delta V_{I_{out}}^I(s)}{\Delta V_{Q_{out}}^I(s)} = \frac{1}{sR_1 C_1}. \quad (8)$$

According to (8), the output signals have exactly the same magnitude at the single angular frequency of $\omega_l = 1/R_1 C_1$. Furthermore, (8) is purely imaginary ($s = i\omega$). Thus, the phase difference between I and Q outputs is exactly 90° with all frequencies and with all R_l and C_l values. In addition, the result is independent of the load impedance if identical load impedance at every output node is assumed.

A wider amplitude balance with Type I PPF is achieved by cascading several stages. For example, the transfer functions of

I and Q channels of a two-stage Type I PPF are calculated with (4):

$$H_{2\text{-stg},I}^I(s) = \frac{\Delta V_{Iout}^I}{\Delta V_{Iin}^I} = \frac{Z_{L1}Z_{L2}(1-s^2C_1R_1C_2R_2)}{(R_1+Z_{L1}+sC_1R_1Z_{L1})(R_2+Z_{L2}+sC_2R_2Z_{L2})}, \quad (9)$$

$$H_{2\text{-stg},Q}^I(s) = \frac{\Delta V_{Qout}^I}{\Delta V_{Iin}^I} = \frac{Z_{L1}Z_{L2}s(C_1R_1+C_2R_2)}{(R_1+Z_{L1}+sC_1R_1Z_{L1})(R_2+Z_{L2}+sC_2R_2Z_{L2})}. \quad (10)$$

The amplitude balance then becomes

$$A_{bal,2\text{-stg}}^I = \frac{|H_{2\text{-stg},I}^I(s)|}{|H_{2\text{-stg},Q}^I(s)|} = \frac{1+\omega^2R_1C_1R_2C_2}{\omega(R_1C_1+R_2C_2)}. \quad (11)$$

Thus, unity gain balance is achieved at $\omega_1=1/R_1C_1$ and $\omega_2=1/R_2C_2$. In addition, the phase balance is always 90° at all frequencies, R and C values, and load impedances. For higher order PPFs the transfer functions can be calculated similarly.

Next, we will repeat the previous analysis for Type II PPF. The output voltages can be calculated in a similar manner as for Type I PPF but in this case the Q input signals are $V_{Qin-}=V_{Iin+}$ and $V_{Qin+}=V_{Iin-}$ for the first stage. The transfer functions of the single-stage Type II PPF are

$$H_{1\text{-stg},I}^{II}(s) = \frac{Z_{L1}}{R_1+Z_{L1}+sR_1C_1Z_{L1}}(1-sC_1R_1), \quad (12)$$

$$H_{1\text{-stg},Q}^{II}(s) = \frac{Z_{L1}}{R_1+Z_{L1}+sR_1C_1Z_{L1}}(1+sC_1R_1). \quad (13)$$

The ratio of I and Q outputs is

$$\frac{H_{1\text{-stg},I}^{II}(s)}{H_{1\text{-stg},Q}^{II}(s)} = \frac{1-sR_1C_1}{1+sR_1C_1}. \quad (14)$$

Thus, the amplitude balance is unity with all component R_i and C_i values, all frequencies, and load impedances but the *phase* is exactly 90° only at $\omega_1=1/R_1C_1$. For a two-stage Type II PPF the transfer functions are

$$H_{2\text{-stg},I}^{II}(s) = \frac{Z_{L1}Z_{L2}(1-s(C_1R_1+C_2R_2)-s^2C_1R_1C_2R_2)}{(R_1+Z_{L1}+sC_1R_1Z_{L1})(R_2+Z_{L2}+sC_2R_2Z_{L2})}, \quad (15)$$

$$H_{2\text{-stg},Q}^{II}(s) = \frac{Z_{L1}Z_{L2}(1+s(C_1R_1+C_2R_2)-s^2C_1R_1C_2R_2)}{(R_1+Z_{L1}+sC_1R_1Z_{L1})(R_2+Z_{L2}+sC_2R_2Z_{L2})}. \quad (16)$$

The ratio between I and Q outputs is

$$\frac{H_{2\text{-stg},I}^{II}(s)}{H_{2\text{-stg},Q}^{II}(s)} = \frac{1-s(R_1C_1+R_2C_2)-s^2R_1C_1R_2C_2}{1+s(R_1C_1+R_2C_2)-s^2R_1C_1R_2C_2}. \quad (17)$$

The previous analyzes can be extended for higher order PPFs as well. It turns out that Type II PPF has always unity amplitude balance and the phase is 90° only at each RC pole. Respectively, Type I PPF has ideal phase balance and amplitude balance is unity at each RC pole frequency.

III. IMAGE-REJECT RATIO

In this section, image-rejection ratios (IRR) of both PPF topologies are studied. In receiver context IRR is defined as a

relation of the desired sideband to the suppression of image sideband. The IRR was first calculated by Norgaard [16] and it is expressed as

$$IRR = \frac{1+2A_{bal}\cos(\Delta\theta)+A_{bal}^2}{1-2A_{bal}\cos(\Delta\theta)+A_{bal}^2}. \quad (18)$$

In (18) A_{bal} and $\Delta\theta$ define the amplitude ratio of I and Q outputs and phase deviation from an ideal 90° between I and Q branches, respectively. If the IRR is separately defined with magnitude balance (IRR_{gain}) and phase deviation (IRR_{phase}) factors, (18) simplifies to

$$IRR_{gain} = IRR_{\Delta\theta=0} = \left[\frac{1+A_{bal}}{1-A_{bal}} \right]^2, \quad (19)$$

$$IRR_{phase} = IRR_{A_{bal}=1} = \cot^2\left(\frac{\Delta\theta}{2}\right). \quad (20)$$

Thus, the amount of phase and amplitude imbalance provided by a PPF can be converted into equal IRR. Such IRR is a figure-of-merit for a PPF used for I/Q generation.

This section is divided in two parts. The IRR performances of both PPF topologies with equal and unequal RC pole frequencies are studied separately. In the former case, equal component values are utilized in all filter stages and in the latter case the resistor and capacitor values of different stages are adjusted separately.

A. Equal RC Poles

Type I PPF has ideal phase response resulting $IRR=IRR_{gain}$. Based on (8), the amplitude balance is simply $A_{bal}=\omega_1/\omega$, where $\omega_1=1/R_1C_1$. According to (19), the IRR becomes

$$IRR_{gain,1\text{-stg}}^I = \left(\frac{\omega+\omega_1}{\omega-\omega_1} \right)^2. \quad (21)$$

Respectively, Type II PPF has ideal gain balance. Therefore, $IRR = IRR_{phase}$ and solving the phase of (14) and using the definition of (20), the IRR_{phase} becomes

$$IRR_{phase,1\text{-stg}}^{II} = \cot^2\left(\frac{1}{2}\arctan\left(\frac{(\omega-\omega_1)(\omega+\omega_1)}{2\omega\omega_1}\right)\right). \quad (22)$$

It can be proven with trigonometric functions that (22) equals to (21), i.e. the IRR performance is *equal* for both PPF types. That holds for multi-stage PPFs, too. Although both PPF topologies have equal IRR performance, the choice of PPF type may be eventually constrained by amplitude and phase imbalance specifications required by the system.

According to (21) and (22), IRR depends only on pole frequency. Therefore, the IRR of a passive polyphase network cannot be improved by the choice of the topology. For the following IRR analysis, (21) is used.

PPF stages with equivalent R_i and C_i values can be cascaded. The IRR of an n -stage PPF with equal poles is

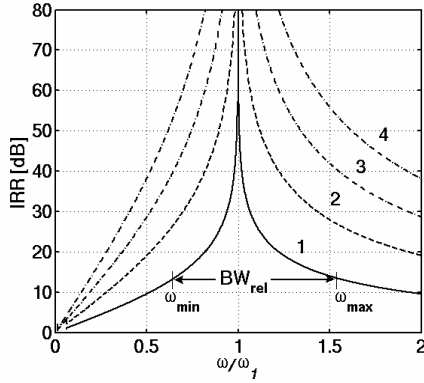


Fig. 4. IRR of equal RC pole PPFs with 1 to 4 stages as a function of frequency. The frequency axis is scaled with respect to $\omega_1=1/R_1C_1$.

$$IRR_{gain,n-stg} = \left(\frac{\omega + \omega_1}{\omega - \omega_1} \right)^{2n}. \quad (23)$$

The IRRs of PPFs with 1 to 4 stages are shown in Fig. 4, where the frequency axis is scaled with respect to ω_1 . The relative bandwidth BW_{rel} , which defines the ratio of maximum and minimum frequencies where a specific IRR is achieved, is shown in Fig. 4 and is defined as

$$BW_{rel} = \frac{\omega_{max}}{\omega_{min}}. \quad (24)$$

The BW_{rel} for an n -stage PPF is calculated as

$$BW_{rel,n-stg} = \left(\frac{IRR^{1/2n} + 1}{IRR^{1/2n} - 1} \right)^2. \quad (25)$$

As a result, the IRR as a function of BW_{rel} becomes

$$IRR = \left(\frac{\sqrt{BW_{rel}} + 1}{\sqrt{BW_{rel}} - 1} \right)^{2n}. \quad (26)$$

Equation (26) directly relates the targeted IRR, BW_{rel} , and the number of PPF stages together. The IRRs of PPFs with 1 to 4 stages are shown in Fig. 5 as a function of relative bandwidth. For example, if the designed PPF should have a BW_{rel} of 2, the minimum IRR increases approximately 15 dB per PPF stage.

B. Two-Stage PPF with Unequal RC Poles

The IRR for a two-stage PPF calculated with (11) and (19) is given by

$$IRR_{2-stg} = \left(\frac{\omega + \omega_1}{\omega - \omega_1} \right)^2 \left(\frac{\omega + \omega_2}{\omega - \omega_2} \right)^2, \quad (27)$$

where $\omega_1=1/R_1C_1$ and $\omega_2=1/R_2C_2$. The corresponding curve is plotted in Fig. 6. For the following analysis, without losing any generality, the pole frequency ω_1 is assumed to be higher than ω_2 . Fig. 6 depicts that with unequal RC poles there is a minimum IRR (IRR_{min}) locating between ω_1 and ω_2 . The minimum IRR frequency is $\omega_{IRR,min}=1/\sqrt{R_1C_1R_2C_2}$. To simplify the following calculations, the ratio of RC poles ω_1 and ω_2 is defined with a pole-splitting factor k_2 as follows:

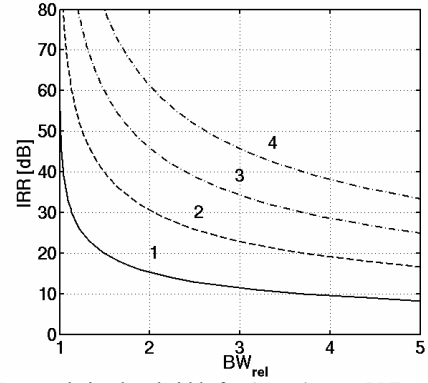


Fig. 5. IRR vs. relative bandwidth for 1- to 4-stage PPFs with equal RC pole frequencies.

$$k_2 = \frac{\omega_1}{\omega_2} = \frac{R_2C_2}{R_1C_1} > 1. \quad (28)$$

Then, the minimum IRR of a two-stage PPF between ω_1 and ω_2 is expressed as

$$IRR_{min,2-stg} = \left(\frac{\sqrt{k_2} + 1}{\sqrt{k_2} - 1} \right)^2. \quad (29)$$

According to (27) the IRR depends only on the RC pole frequencies and according to (29) the minimum IRR is defined by the *ratio* of RC pole frequencies. In a case of equal RC poles ($k_2=1$), (29) goes to infinity, since there is no inter-pole minimum. The corner frequencies $\omega_{c,min}$ and $\omega_{c,max}$ define points, where IRR equal to IRR_{min} is achieved (see Fig. 6)

$$\omega_{c,min\&max} = \frac{\omega_1 (k_2 + 1) \pm (k_2 - 1) \sqrt{k_2^2 + 6k_2 + 1}}{4 k_2 \sqrt{k_2}}. \quad (30)$$

As a result, the relative bandwidth BW_{rel} , where the minimum IRR is reached, is given by

$$BW_{rel,2-stg} = \frac{\omega_{c,max}}{\omega_{c,min}} = \frac{(k_2 + 1)^2 + (k_2 - 1) \sqrt{k_2^2 + 6k_2 + 1}}{(k_2 + 1)^2 - (k_2 - 1) \sqrt{k_2^2 + 6k_2 + 1}}. \quad (31)$$

Therefore, if BW_{rel} is known, k_2 can be expressed as

$$k_2 = \frac{1 + BW_{rel,2-stg} + (\sqrt{BW_{rel,2-stg}} - 1)(\sqrt{BW_{rel,2-stg}} + 1)}{\sqrt{BW_{rel,2-stg}}} - 1. \quad (32)$$

The relation between BW_{rel} and minimum IRR according to (29) for a two-stage PPF is

$$BW_{rel,2-stg} = \frac{(1 + \sqrt{IRR})^2 + 2\sqrt{2}IRR^{1/4}\sqrt{IRR+1}}{(1 + \sqrt{IRR})^2 - 2\sqrt{2}IRR^{1/4}\sqrt{IRR+1}}. \quad (33)$$

When comparing (33) to (25), it can be noted that the BW_{rel} of a 2-stage PPF with unequal poles is always wider compared to PPF with equal poles. However, the difference decreases if a high IRR is required, because then small pole splitting factor k_2 is required. For example, with IRR target of 30 dB and 40 dB the BW_{rel} of unequal poles is approximately 36% and 18% larger than with equal poles, respectively.

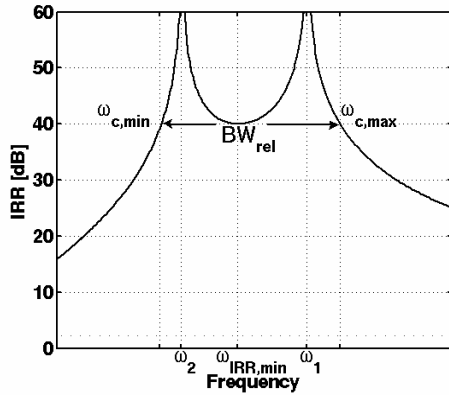


Fig. 6. IRR of a 2-stage PPF. According to (29), an IRR of 40 dB is achieved with pole splitting factor $k_2 = 121/81$.

C. Three-Stage PPF with Unequal RC Poles

For a three-stage PPF, the IRR as a function of frequency is

$$IRR_{3-stg} = \left(\frac{\omega + \omega_1}{\omega - \omega_1} \right)^2 \left(\frac{\omega + \omega_2}{\omega - \omega_2} \right)^2 \left(\frac{\omega + \omega_3}{\omega - \omega_3} \right)^2. \quad (34)$$

Similarly as in two-stage case, the following analysis assumes $\omega_1 > \omega_2 > \omega_3$. The RC poles ω_2 and ω_3 are related to ω_1 with pole splitting factors k_2 and k_3 . k_2 is defined as in (28) and k_3 is

$$k_3 = \frac{\omega_1}{\omega_3} = \frac{R_3 C_3}{R_1 C_1} > 1. \quad (35)$$

When (34) is plotted, two IRR minimum notches between ω_3 and ω_1 are obtained as is shown in Fig. 7. First, such a relation between k_2 and k_3 is calculated, that the minimum IRR (IRR_{min}) of the two notches are equivalent. The IRR_{min} s are *not* located at geometric average frequencies of $\sqrt{\omega_1 \omega_2}$ and $\sqrt{\omega_2 \omega_3}$, but at

$$\omega_{IRRmin} = \frac{\omega_1}{\sqrt{2}} \sqrt{\frac{F_1(k_2, k_3) \pm \sqrt{(k_2+1)(k_2+k_3)(k_3+1)(F_1(k_2, k_3) - 6k_2 k_3)}}{k_2 k_3 (k_2 + k_2 k_3 + k_3)}}, \quad (36)$$

where

$$F_1(k_2, k_3) = k_2(k_2 k_3 + k_2 + 1) + k_3(k_2 k_3 + k_3 + 1). \quad (37)$$

To achieve equivalent IRR_{min} s at those frequencies, there are actually three optimum relations between k_2 and k_3 :

$$k_3 = \frac{1}{k_2}, \quad k_3 = \sqrt{k_2}, \quad \text{and} \quad k_3 = k_2^2.$$

Based on definitions of pole locations, we must have $k_3 > k_2$ and only the last result always obeys this. From here on, the relation according to (38) is used in all calculations.

$$k_3 = k_2^2. \quad (38)$$

The exact IRR_{min} formula at frequencies according to (36) becomes far too complicated to present here, though it can be calculated and included into a design formula set. To simplify the calculations, IRR minimum presented here is calculated at geometric average of RC poles to achieve simpler equation. As a result, an IRR minimum of a three stage PPF is

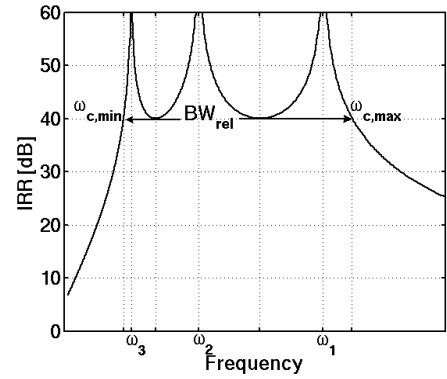


Fig. 7. IRR of a 3-stage PPF. An IRR of 40 dB is achieved with pole splitting factor $k_2 \approx 1.84$ and $k_3 = k_2^2 \approx 3.39$.

$$IRR_{min,3-stg} = \left(\frac{\sqrt{k_2} + 1}{\sqrt{k_2} - 1} \right)^3 \left(\frac{k_2 - \sqrt{k_2} + 1}{k_2 + \sqrt{k_2} + 1} \right). \quad (39)$$

Equation (39) slightly overestimates the IRR compared to the exact calculated IRR minimum. The maximum error is approximately 0.23 dB when k_2 is close to unity and decreases with larger k_2 . Thus, the error is insignificant and (39) can be used to calculate k_2 if IRR target is known. Due to the lack of closed-form solution of quintic formula, k_2 can not be analytically solved from (39). Therefore, a rough value for k_2 can be sketched from Fig. 8 or k_2 can be calculated numerically.

Next, the relative bandwidth of a 3-stage PPF is calculated. The frequencies $\omega_{c,min}$ and $\omega_{c,max}$ shown in Fig. 7 present corner frequencies, where the IRR_{min} is achieved and are given as

$$\omega_{c,min} = \frac{\omega_3}{2\sqrt{k_2}} \frac{(1+k_2)^2(1+k_2^2) - \sqrt{F_2(k_2)}}{(2+k_2+k_2^2)}, \quad (40)$$

$$\omega_{c,max} = \frac{\omega_1}{2k_2\sqrt{k_2}} \frac{(1+k_2)^2(1+k_2^2) + \sqrt{F_2(k_2)}}{(1+k_2+2k_2^2)}, \quad (41)$$

where $\omega_1 = 1/R_1 C_1$, $\omega_3 = \omega_1/k_2^2$, and

$$F_2(k_2) = 1 + 4k_2 - 10k_2^4 + 4k_2^7 + k_2^8. \quad (42)$$

The relative bandwidth calculated with (40) and (41) is approximated with the following formula, so that k_2 can be easily solved if BW_{rel} is known

$$BW_{rel,3-stg} \approx 2k_2^2 - 1.9k_2 + 0.9. \quad (43)$$

Equation (43) predicts the exact relative bandwidth with an accuracy better than 1.5 % when $k_2 < 2.8$. The IRR_{min} and the relative bandwidth, where IRR_{min} is covered, are shown as a function of k_2 in Fig. 8. For example, to achieve better than 40-dB IRR, k_2 shall not exceed 1.84. Then, the BW_{rel} becomes approximately 4.2, which is a significant improvement compared to the BW_{rel} of a two-stage PPF (1.78) with the same IRR. IRR as a function of relative bandwidth for 2-, 3-, and 4-stage PPFs is shown in Fig. 9.

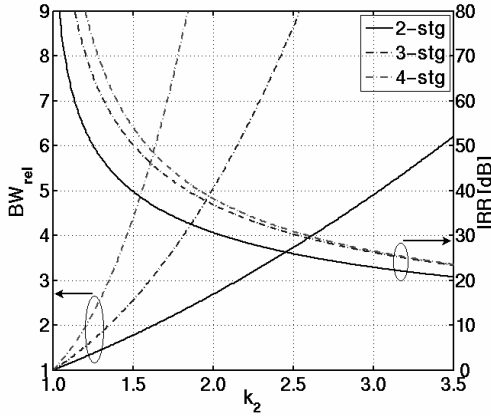


Fig. 8. IRR and relative bandwidth BW_{rel} as a function of pole splitting factor k_2 . The optimum pole splitting is calculated according to (38) and (B.5) for 3- and 4-stage PPFs, respectively.

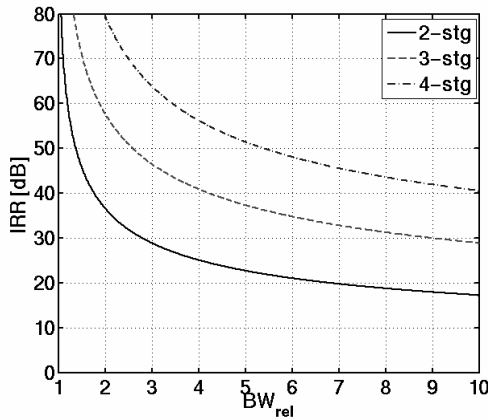


Fig. 9. IRR as a function of relative bandwidth BW_{rel} for 2-, 3-, and 4-stage PPFs with unequal RC pole frequencies.

D. Optimal Pole Splitting of Higher Order PPFs

An n -stage PPF with unequal RC poles has $n-1$ IRR minimum notches. When equivalent IRR_{min} s are targeted, the optimum RC pole frequencies for PPFs having more than three stages are not achieved with a generic formula of $k_n/k_{n-1}=k_2$ ($n>3$). For example, the calculation of an optimal four-stage PPF is presented in Appendix B.

IV. INTRINSIC PPF LOSS

When PPFs are used for quadrature signal generation in the LO signal path, the loss due to PPF is usually compensated with on-chip buffers. Often, the current consumption of the LO buffers becomes a remarkable part of RF front-end power budget. Therefore, it is crucial to be aware of the methods to minimize the PPF loss. As a thumb of rule, the loss due to PPF is usually estimated to be 3 dB/stage. That holds, when all PPF stages have equal RC poles, the loss is calculated at $\omega=1/RC$, and the PPF is terminated with infinite load impedance.

The previous section described the optimization of IRR bandwidth. The analysis showed that there was no difference in IRR performance between Type I and II PPFs. In this section, the loss of both PPF types is analyzed as a function of number of stages and pole splitting factor. In addition, in a case of multi-stage PPF, the optimal device scaling is

discussed. In the following analysis, the source impedance is assumed zero and the termination impedance of the last PPF stage is infinite. This section discusses the loss caused by the PPF only, i.e. *intrinsic* loss. The effect of the finite input and output impedances are considered in Section V.

A. Loss of Single-Stage PPFs

The differential output signals of a single-stage PPF is calculated from (4) by setting $Z_{L1}=\infty$. In a case of Type I PPF, I and Q output voltages have low-pass and high-pass frequency characteristics, respectively. The outputs have an equal magnitude at $\omega_l=1/R_1C_1$ calculated as

$$H_{1-stg,\omega_l}^I = \left. \frac{1}{1+sC_1R_1} \right|_{s=i/R_1C_1} = \frac{1}{2}|1-i| = \frac{1}{\sqrt{2}}, \quad (44)$$

which corresponds to 3-dB loss. For the Type II PPF the loss at ω_l is given by

$$H_{1-stg,\omega_l}^{II} = \left. \frac{1-sC_1R_1}{1+sC_1R_1} \right|_{s=i/R_1C_1} = |-i| = 1, \quad (45)$$

which is 3 dB less than the loss of Type I PPF.

B. Loss of Two-Stage PPFs

The loss for two-stage Type I PPF can be calculated by cascading (4) for $n=1$ and $n=2$ and by applying

$$Z_{L1} = \frac{R_2 + Z_{L2} + sC_2R_2Z_{L2}}{1 + sC_2(R_2 + 2Z_{L2})} \xrightarrow{Z_{L2} \rightarrow \infty} \frac{1}{2} \left(R_2 + \frac{1}{sC_2} \right) \quad (46)$$

for the load impedance Z_{L1} of the first PPF stage. The last form of (46) is used in the following analysis, because Z_{L2} is infinite. In the case of Type I PPF, the I-output has a loss maximum and the Q-output has a loss minimum at the geometric average of the RC poles, i.e. $\omega=1/\sqrt{R_1C_1R_2C_2}$, as is shown in Fig. 10. At that frequency, the I and Q output losses become

$$L_{2-stg,I,max}^I = \frac{(C_1R_1 + 2C_2R_1 + R_2C_2)^2}{4C_1C_2R_1R_2}, \quad (47)$$

$$L_{2-stg,Q,min}^I = \frac{(C_1R_1 + 2C_2R_1 + R_2C_2)^2}{C_1R_1 + C_2R_2}, \quad (48)$$

respectively. In the case of equal RC poles, (47) and (48) will lead to 6-dB loss (i.e. 3 dB/stage) at both outputs. However, in a general case, RC poles are not equal. It is possible to design the pole ω_2 to the wanted frequency with the pole splitting parameter k_2 by scaling either the value of R_2 or C_2 or both. Since the minimum (or maximum) loss is a function of R_1 , C_1 , R_2 , and C_2 as is shown in (47) and (48), there are optimal component values, which minimize the PPF loss. To calculate the optimum device scaling, the parameter k_2 is further divided into two parts

$$k_2 = k_{2R}k_{2C}, \quad (49)$$

where k_{2R} and k_{2C} denote the ratio of the first and second stage resistors and capacitors, i.e. $k_{2R}=R_2/R_1$ and $k_{2C}=C_2/C_1$. Equation (47) can be modified into

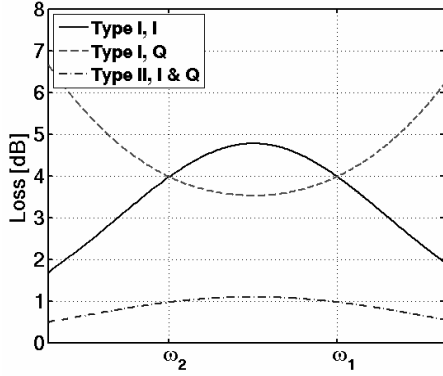


Fig. 10. Loss of two-stage PPFs as a function of frequency. The loss is shown for both PPF types. Here, the pole splitting factor $k_2=3$ ($k_{2R}=3$ and $k_{2C}=1$) was chosen since it is a typical value in a practical PPF.

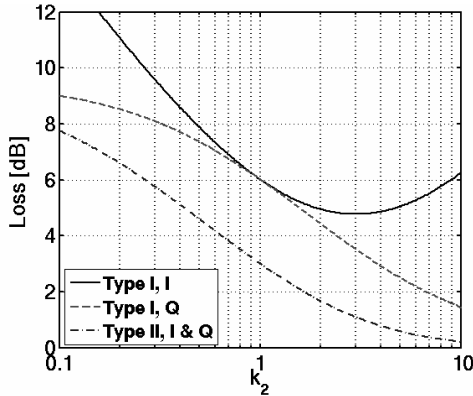


Fig. 11. Maximum loss of both PPF types as a function of pole splitting factor k_2 . Equal capacitor values are used in both stages. For Type I PPF, both the I and Q outputs are shown separately.

$$L'_{2-stg,I,max} = \frac{(1+2k_{2C}+k_{2C}k_{2R})^2}{4k_{2C}k_{2R}} = \frac{(1+2k_{2C}+k_2)^2}{4k_2}. \quad (50)$$

According to the last form, if k_2 is fixed, for example due to IRR requirement, the loss is minimized when k_{2C} is as small as possible. In other words, when the component values of the lower pole ω_2 are chosen, the resistor value should be larger and capacitor value smaller compared to the component values of the higher pole ω_1 (i.e. $R_2 > R_1$ and $C_2 < C_1$). This holds also for higher order PPFs. In practice, when a PPF with unequal RC poles is designed, it is beneficial to dimension all the capacitors with a fixed value. Then, $k_{2C}=1$ and the pole splitting factor k_2 is defined by the resistor ratio k_{2R} only. The following analysis is performed for cases, where equal capacitor values are used in all stages, i.e. $k_{2C}=1$ if not otherwise mentioned. Then, the losses for Type I PPF I and Q outputs as a function of k_2 are achieved by

$$L'_{2-stg,I,max} = \frac{(k_2+3)^2}{4k_2}, \quad (51)$$

$$L'_{2-stg,Q,min} = \left(\frac{k_2+3}{k_2+1} \right)^2, \quad (52)$$

respectively. The losses of both outputs are plotted in Fig. 11 as a function of k_2 . With equal RC poles ($k_2=1$), both (51) and

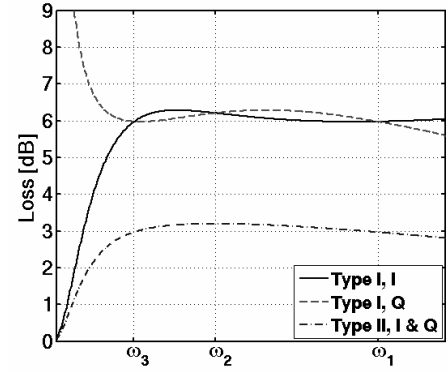


Fig. 12. Loss of three-stage PPFs as a function of frequency. Loss is shown for both PPF types. The pole splitting factor $k_2=2$.

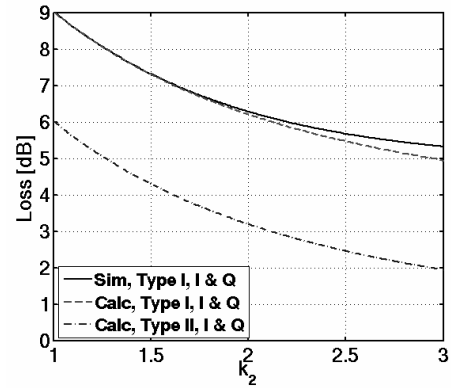


Fig. 13. Loss of three-stage PPF at ω_2 as a function of pole splitting factor k_2 . Loss of PPF types I and II are calculated according to (54) and (55), respectively. The simulated minimum loss of PPF Type I is also shown.

(52) lead to loss of 6 dB. In addition, it is observed, that $k_2 \geq 1$ is required to minimize the losses. Therefore, the RC poles should be placed such that the highest RC pole is the first stage in the signal path, i.e. the impedance level increases along with signal path. Then, the average loss is *less* than 3 dB/stage.

Next, the similar analysis is carried out for Type II PPF. According to (17), I and Q outputs of a two-stage Type II PPF always have balanced amplitude. As is shown in Fig. 10, the maximum loss is achieved at $\omega=1/\sqrt{R_1C_1R_2C_2}$ and it is

$$L''_{2-stg,max} = \frac{(C_1R_1+2C_2R_1+R_2C_2)^2}{C_1^2R_1^2+6C_1R_1C_2R_2+C_2^2R_2^2} = \frac{(1+2k_{2e}+k_2)^2}{1+6k_2+k_2^2}. \quad (53)$$

The loss is minimized by choosing the capacitor scaling factor k_{2C} as small as possible. The loss of Type II PPF is plotted in Fig. 11 as a function of k_2 , and $k_{2C}=1$. When $k_2=1$, the loss becomes 3 dB. The loss does not have optimum point as a function of k_2 and it approaches 0 dB when k_2 increases.

C. Loss of Three-Stage PPFs

The losses of three-stage PPFs as a function of frequency are shown in Fig. 12, where $k_2=k_{2R}=2$, and $k_{3C}=k_{2C}=1$. Both the I and Q outputs of Type I PPF have loss maximums between ω_1 and ω_3 . The frequencies of loss maximums are too lengthy to present here as closed-form formulas. Therefore, the loss of 3-stage PPF is calculated at $\omega_2=1/R_2C_2$, which is the geometric average of ω_1 and ω_3 . At that frequency the loss becomes

$$L_{3\text{-stg},\omega_2}^I = 2 \left(1 + \frac{4}{(1+k_2)^2} \right)^2. \quad (54)$$

The calculated and simulated loss minimums are plotted in Fig. 13 as a function of k_2 . Loss is reduced with increased pole splitting. When $k_2 < 2$, (54) predicts the loss of Type I with an accuracy better than 0.1 dB.

The PPF Type II has a loss minimum exactly at ω_2 and it is expressed as

$$L_{3\text{-stg},\omega_2}^{II} = \left(1 + \frac{4}{(1+k_2)^2} \right)^2. \quad (55)$$

Comparison of (54) and (55) reveals that the intrinsic loss of Type II PPF is 3 dB smaller than that of Type I at ω_2 . The 3-dB difference in loss between PPF types is achieved at every pole frequency independent of the number of stages.

V. THE EFFECT OF TERMINATION IMPEDANCES

In this section the effects of input and output impedances to the PPF loss are analyzed. Finite termination impedances cause voltage division both at the input and output of the PPF. In previous sections the optimal pole frequencies and device scaling were analyzed. The analysis so far, however, does not define, which resistor and capacitor values should be chosen for the PPF. This chapter shows how the impedance level of the PPF should be chosen to minimize the overall loss if finite source (Z_S) and load impedances (Z_L) are known a priori. In addition, the optimum impedance level depends on the PPF topology and on the number of stages.

A. Optimum Component Values for a Single-Stage PPF

The differential input impedance of a Type I PPF is

$$Z_{in,1\text{-stg}}^I = 2 \frac{R_1 + Z_{L1} + sC_1 R_1 Z_{L1}}{1 + sC_1 (R_1 + 2Z_{L1})}, \quad (56)$$

where Z_{L1} is the load impedance of a single output node (see Fig. 3a). The output impedance can be calculated with (56) by replacing Z_{L1} with Z_S . In a case of PPF Type I, the differential input and output impedance simplifies to $R_1 + 1/sC_1$ at the pole frequency of $\omega_l = 1/R_1 C_1$. The result is independent of Z_{L1} or Z_S .

In a general case, the signal loss due to voltage division at the input and output are calculated as

$$L_{input} = \frac{V_{in,PPF}}{V_{source}} = \left| \frac{Z_{in,PPF}}{Z_{in,PPF} + Z_S} \right|, \quad (57)$$

$$L_{output} = \frac{V_{load}}{V_{out,PPF}} = \left| \frac{Z_L}{Z_{out,PPF} + Z_L} \right|, \quad (58)$$

where $Z_{in,PPF}$ and $Z_{out,PPF}$ are differential input and output impedances of the PPF and Z_S and Z_L are differential source and load impedances, respectively. When Z_S is finite, the voltage division at the input is minimized by maximizing the value of R_1 . However, for the minimal voltage division at the output the value of R_1 should be minimized when Z_L is finite.

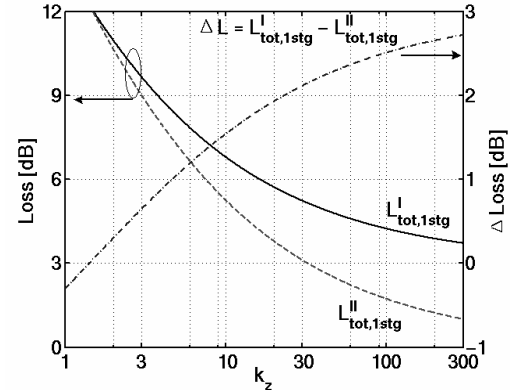


Fig. 14. Overall loss of a single-stage PPF. Loss is shown for both PPF types as a function of k_Z (ratio of output and input impedances). In right y-axis, the difference of the losses is shown.

Thus, there is an optimum PPF impedance level, which minimizes the overall loss. The absolute values of Z_S and Z_L are related to the resistor value R_1 of the first PPF stage with parameters k_S and k_L :

$$|Z_S| = \frac{R_1}{k_S}, \quad |Z_L| = R_1 k_L. \quad (59)$$

A parameter k_Z is used to relate the output and input impedances.

$$\frac{|Z_L|}{|Z_S|} = k_S k_L = k_Z \quad (60)$$

As was shown earlier, the intrinsic PPF loss does not depend on the component values. Therefore, for a single-stage PPF, the optimum impedance level can be calculated by setting voltage divisions L_{input} and L_{output} equal. For Type I PPF the optimum output impedance relation k_L becomes

$$k_{L,opt,1\text{-stg}}^I = \sqrt{2 \frac{|Z_L|}{|Z_S|}} = \sqrt{2k_Z}. \quad (61)$$

The optimum R_1 can then be calculated using (59). It should be noticed that $Z_{in,PPF}$, $Z_{out,PPF}$, Z_S , and Z_L are differential, when using equations above.

Due to the dual feed structure, the input impedance of the PPF Type II is half of input impedance of (56). When the analysis is repeated, the optimum k_L becomes

$$k_{L,opt,1\text{-stg}}^{II} = \sqrt{k_Z}. \quad (62)$$

The optimum impedance level of Type I PPF is $\sqrt{2}$ times larger than of Type II PPF. Therefore, if k_Z is known, the resistor value R_1 of Type II PPF should be $\sqrt{2}$ times larger than in PPF Type I. Accordingly, to maintain pole frequency ω_l the capacitor value C_1 of PPF Type II is $\sqrt{2}$ smaller than in PPF Type I.

The total losses of single-stage Type I and Type II PPFs taking into account both the intrinsic PPF loss and termination losses are expressed as a function of k_Z as

$$L_{tot,1\text{-stg}}^I = \left(\frac{\sqrt{2} + 2\sqrt{k_Z} + \sqrt{2k_Z}}{k_Z} \right)^2, \quad (63)$$

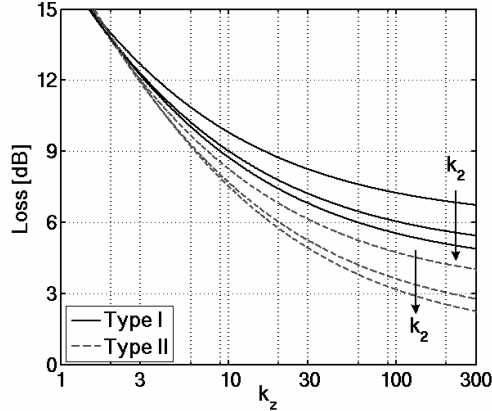


Fig. 15. Overall loss of a two-stage PPF. Loss is shown for both PPF types as a function of termination impedance ratio k_Z . The pole splitting factor k_2 has values of 1, 2, and 3. The arrow shows the direction of increasing k_2 .

$$L_{tot,1-stg}^{II} = \left(\frac{2 + 2\sqrt{k_Z + k_Z}}{k_Z} \right)^2, \quad (64)$$

respectively. The total losses and the difference of the losses are plotted as a function of k_Z in Fig. 14. Due to finite input and output impedances, the difference between loss performance of PPF types is less than 3 dB.

B. Optimum Component Values for Multiple-Stage PPFs

The optimization of a two-stage Type I PPF is first considered. When the input and output impedances are calculated, it turns out that the differential input impedance of PPF Type I at ω_l is $R_1 + 1/sC_1$ regardless of the number of PPF stages. With multi-stage PPF, the input impedance at ω_2 is

$$Z_{in,\omega_2} = \frac{R_2 \left[(C_1 R_1 + C_2 R_2)^2 + 2R_1 R_2 (C_1^2 + C_2^2) \right]}{C_1^2 (R_1 + R_2)^2 + R_2^2 (C_1 + C_2)^2} - i \frac{R_2 \left[(C_1 R_1 + C_2 R_2)^2 + 2C_1 C_2 (R_1^2 + R_2^2) \right]}{C_1^2 (R_1 + R_2)^2 + R_2^2 (C_1 + C_2)^2}. \quad (65)$$

At ω_2 the output impedance of PPF Type I (Z_{out,ω_2}) is $R_2 + 1/sC_2$ and at ω_l the output impedance Z_{out,ω_l} can be achieved with (65) by switching $R_1 \leftrightarrow R_2$ and $C_1 \leftrightarrow C_2$.

In the analysis of intrinsic PPF loss we learnt that it is favorable to perform the pole splitting by scaling the resistor values to minimize the loss. Therefore, k_2 is again divided into two parts ($k_2 = k_{2R} k_{2C}$) to find both optimal component values and scaling ratio when finite termination impedances are taken into account. The optimum loss is found by making overall input and output voltage divisions at ω_l and ω_2 equal. This results in the following equation:

$$\left| \frac{Z_{in,\omega_l}}{Z_{in,\omega_l} + Z_S} \right| \left| \frac{Z_L}{Z_L + Z_{out,\omega_l}} \right| = \left| \frac{Z_{in,\omega_2}}{Z_{in,\omega_2} + Z_S} \right| \left| \frac{Z_L}{Z_L + Z_{out,\omega_2}} \right|. \quad (66)$$

For simplicity, termination impedances Z_S and Z_L are assumed frequency independent. Equation (66) results an optimum k_L as

$$k_{L,opt,2-stg}^I = \sqrt{2k_{2R}k_Z}, \quad (67)$$

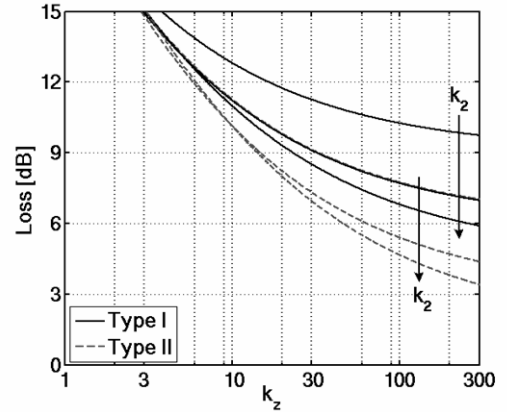


Fig. 16. Overall loss of a three-stage PPF. Loss is shown for both PPF types as a function of k_Z . The pole splitting factor k_2 has values 1, 2, and 3. The result $k_2=1$ for Type II overlaps with $k_2=2$ for Type I. The arrow shows the direction of increasing k_2 .

Similar analysis can be derived for Type II PPF too, and then

$$k_{L,opt,2-stg}^{II} = \sqrt{k_{2R}k_Z}. \quad (68)$$

When the overall PPF loss is calculated with the result given by (67), the analysis again shows that pole splitting is beneficial to perform by increasing the resistor values. Therefore, the loss of the whole two-stage PPF is shown in Fig. 15 in a case, where $k_{2C} = 1$, and resistor values (k_{2R}) are increased from 1 to 3. The Type II PPF has typically 1-2 dB lower loss than Type I PPF and the difference between PPF losses decreases with small k_Z values.

Finally, the loss of a three-stage PPF is considered. For a Type I PPF, the I and Q outputs signals are balanced at ω_l , ω_2 , and ω_3 . The optimum component values are achieved when voltage divisions due to termination impedances are equal at ω_l and ω_3 similarly as in (66). Then, the optimum k_L values for Type I and II PPFs are calculated with

$$k_{L,opt,3-stg}^I = k_{2R} \sqrt{2k_Z}, \quad (69)$$

$$k_{L,opt,3-stg}^{II} = k_{2R} \sqrt{k_Z}, \quad (70)$$

respectively. Therefore, the optimum input impedance of PPF Type II is $\sqrt{2}$ smaller than of Type I PPF for 1-, 2-, and 3-stage PPFs. The optimal total loss of a 3-stage PPF as a function of k_Z is shown Fig. 16 for both filter types. The loss is shown in a case, where $k_{2C} = 1$, and resistor values ($k_2 = k_{2R}$) of 1, 2, and 3.

VI. THE EFFECT OF PARASITIC CAPACITANCE

The realistic monolithic components always have parasitic capacitance to the substrate. For simplicity, in the following analysis the parasitic capacitances of the PPF components are combined into a single parasitic capacitor C_{par} . In addition, it is assumed that the value of C_{par} is equal for each PPF node. Precisely speaking, this is not exactly true since larger resistors of small-valued devices implemented using several parallel resistors introduce more parasitic capacitance. However, the main contributor of parasitic capacitance is the capacitor of the RC pole, and in a well-designed PPF these are equal in each

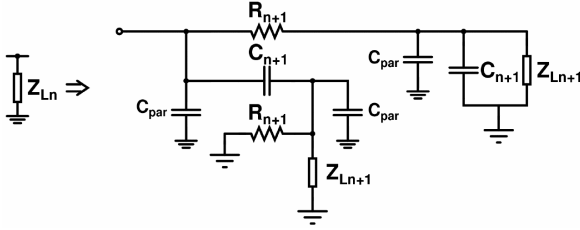


Fig. 17. The equivalent load network for calculation of PPF with parasitic capacitance.

stage. Thus, the error introduced by setting C_{par} fixed is small.

The output signals of n^{th} PPF stage are now expressed as

$$\begin{bmatrix} \Delta V_{Iout,n} \\ \Delta V_{Qout,n} \end{bmatrix} = \frac{Z_{Ln}}{R_n + Z_{Ln} + sR_n Z_{Ln} (C_n + C_{par})} \begin{bmatrix} 1 & -sC_n R_n \\ sC_n R_n & 1 \end{bmatrix} \begin{bmatrix} \Delta V_{In,n} \\ \Delta V_{Qin,n} \end{bmatrix}. \quad (71)$$

The load impedance Z_{Ln} is calculated from a network depicted in Fig. 17 and the corresponding formula is given in (72).

$$Z_{Ln,Cpar} = \frac{R_{n+1} + Z_{Ln+1} + sC_{n+1} R_{n+1} Z_{Ln+1} + sC_{par} R_{n+1} Z_{Ln+1}}{1 + sC_{n+1} (R_{n+1} + 2Z_{Ln+1}) + sC_{par} (R_{n+1} + 2Z_{Ln+1} + s2C_{n+1} R_{n+1} Z_{Ln+1} + sC_{par} R_{n+1} Z_{Ln+1})} \quad (72)$$

The C_{par} is in parallel with the load impedance Z_L . As was calculated in (8) and (14), the load impedance does not have an effect on IRR. If the value of C_{par} is equal at each PPF node, it does not affect the IRR either. Therefore, only the loss caused by the parasitic capacitance C_{par} needs to be studied in this section. The amount of extra loss due to C_{par} is similar for both I and Q outputs of Type I PPF. It can be noted that C_{par} causes the same amount of loss for both PPF types, too. The effects of C_{par} on intrinsic loss and voltage division due to finite termination impedances are considered separately. Furthermore, how the C_{par} affects on optimal device values is briefly discussed.

A. Single-Stage PPF

For a single-stage PPF the additional intrinsic loss at $\omega_l = 1/R_l C_l$ is

$$L_{Cpar,1-stg} = \frac{1}{2} \left(\frac{C_1^2 + (C_1 + C_{par})^2}{C_1^2} \right) = \frac{1}{2} (1 + k_{par}^2), \quad (73)$$

where

$$k_{par} = \frac{C_1 + C_{par}}{C_1} = 1 + \frac{C_{par}}{C_1}. \quad (74)$$

For example, a 10-% relative parasitic capacitance causes approximately 0.45-dB additional loss. In addition, C_{par} decreases the input impedance of PPF at ω_l . Due to lower PPF input impedance, the voltage division at the input increases. Additional loss caused by voltage division at the input is

$$L_{Cpar,in} = \left(1 + \frac{C_{par} (2C_1 + C_{par})}{2C_1^2 (1 + 2k_2 + 2k_S^2)} \right) = \left(1 + \frac{(k_{par}^2 - 1)}{2(1 + 2k_2 + 2k_S^2)} \right), \quad (75)$$

where k_S denotes the relation between R_l and differential source impedance according to (59). For example, with $k_S = 1$ a

10-% relative parasitic capacitance causes less than 0.1 dB additional loss at input. In practice, $k_S > 1$ and therefore $L_{Cpar,in}$ has an insignificant effect compared to (73).

The parasitic capacitance decreases also the output impedance, which improves the voltage division at the output. The additional output voltage division due to C_{par} is less than 1 according to

$$L_{Cpar,out} = \left(1 - 2 \frac{k_{par}^2 - 1}{k_{par}^2 + 1} \frac{(1 + k_L)}{(2 + 2k_L + k_L^2)} \right). \quad (76)$$

In (76) k_L is defined according to (59). Also (76) is quite insignificant compared to (73) if $k_L > 10$. Actually, by using optimal k_L values given by (61) and (62), it can be shown that when the effect of losses $L_{Cpar,out}$ and $L_{Cpar,in}$ are combined, the result is always less than unity, i.e. parasitic capacitance decreases the termination losses. Therefore, as a worst case, the loss due to C_{par} can be predicted by (73).

B. Effect on Optimal Device Values

In addition to the increased loss, the C_{par} modifies the optimal component values calculated with (61) and (62). The analysis of the optimal component values due to C_{par} using closed-form expressions is complicated. Therefore, the effect of C_{par} is presented by simulation results. First, the C_{par} is divided into dependent and independent parts of C_l as

$$C_{par} = \theta C_l + C_{fixed}. \quad (77)$$

θ denotes the relative parasitic capacitance of C_l (per plate) and C_{fixed} presents the fixed parasitic capacitance of resistors and metal wiring of the layout etc. The effect of C_{par} was studied in two extreme cases: C_{par} is dependent only on C_l or C_{par} is independent of C_l . In the former case, decreasing the value of C_l and increasing the value of R_l minimizes the overall PPF loss. This is quite understandable because then C_{par} minimizes along with C_l . In the latter case, it is optimal to increase the value of C_l and decrease the value of R_l . This results from (73), which suggest that the value of C_l should be increased compared to C_{par} to minimize the k_{par} and additional intrinsic loss. In a realistic case, C_{par} has both independent and dependent parts of C_l and thus a starting point for finding the optimal component values are given by (61) and (62). This holds for the higher order PPFs, too.

C. Multi-Stage PPFs

The loss caused by parasitic capacitance to a two-stage PPF is considered next. Only the intrinsic PPF loss is analyzed. As was shown for the single-stage PPF, it gives the worst case assumption. The additional loss as a function of frequency can be calculated with

$$L_{Cpar,2-stg}(\omega) = 1 + \frac{(k_{par}^2 - 1) \left(\frac{\omega}{\omega_l} \right)^2 \left[9 + 2k_2 + k_2^2 + 4k_2^2 k_{par}^2 \left(\frac{\omega}{\omega_l} \right)^2 \right]}{1 + (9 + 4k_2 + k_2^2) \left(\frac{\omega}{\omega_l} \right)^2 + k_2^2 \left(\frac{\omega}{\omega_l} \right)^4}, \quad (78)$$

where $\omega_l = 1/R_l C_l$ and k_{par} is calculated according to (74). In

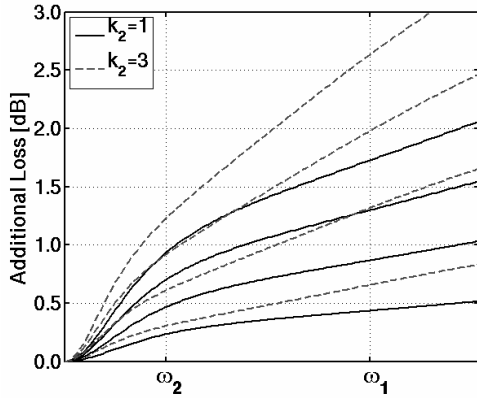


Fig. 18. Additional loss due to C_{par} of a two-stage PPF as a function of frequency. In the first case, no pole splitting is utilized (double RC pole at ω_l) and in the second case PPF was designed with pole splitting of $k_2=3$. The C_{par} values used in plotting were 5%, 10%, 15%, and 20% of C_I .

Fig. 18 (78) is plotted in two cases as a function of frequency. In the first case, no pole splitting is utilized ($k_2=1$, double RC pole at ω_l) and in the second case pole splitting with $k_2=3$ was utilized. Fig. 18 was plotted with C_{par} values being 5%, 10%, 15%, and 20% of C_I . The figure depicts that the additional intrinsic loss of the PPF increases along with the frequency. In addition, the pole splitting enhances the additional loss. The following analysis concentrates on calculating the loss at the highest pole ω_l , where the worst-case results are achieved.

At ω_l and without pole splitting ($k_2=1$) the additional loss due to C_{par} is

$$L_{C_{par},2-stg,\omega=\omega_l,k_2=1} = \frac{1}{4}(1+k_{par}^2)^2, \quad (79)$$

which is familiar from (73). Actually, it can be calculated that the loss of an n -stage PPF at ω_l and with equal RC poles is

$$L_{C_{par},n-stg,\omega=\omega_l,k_2=1} = \frac{1}{2^n}(1+k_{par}^2)^n. \quad (80)$$

Taking into account $k_2 > 1$, the additional loss for a two-stage PPF at ω_l can be calculated as

$$L_{C_{par},2-stg,\omega=\omega_l,k_2>1} = 1 + \frac{1}{2}(k_{par}^2 - 1) \frac{9 + 2k_2 + k_2^2 + 4k_{par}^2 k_2^2}{5 + 2k_2 + k_2^2}. \quad (81)$$

For the higher-order PPFs similar equations become quite lengthy and only simulated result is presented. The additional loss due to C_{par} at ω_l is shown in Fig. 19 as a function of k_2 for 2- and 3-stage PPFs. The parasitic capacitance has values of 5%, 10%, 15%, and 20% of C_I . The loss of 3-stage PPF worsens quite badly along with pole splitting.

D. Summary of Effect of Parasitic Capacitance

In this section, the effect of parasitic capacitance was analyzed with some simplifying assumptions. It was found, that if there is equal parasitic capacitance at each PPF stage output node, it does not affect the IRR performance. Because C_{par} modifies the input and output impedances of PPF, the optimal component values also change in a minor way. In addition, C_{par} increases the intrinsic loss, which worsens at higher frequencies and with pole splitting.

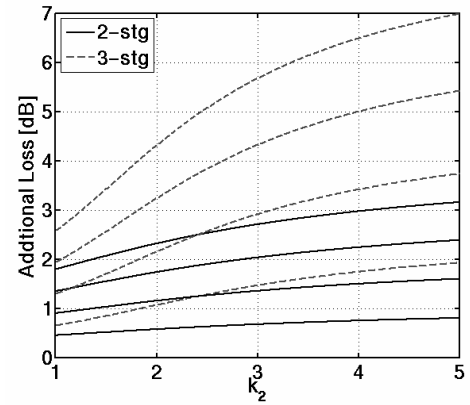


Fig. 19. Additional loss due to C_{par} of a 2- and 3-stage PPFs at ω_l as a function of pole splitting factor k_2 . The parasitic capacitance used in figure were 5%, 10%, 15%, and 20% of C_I .

VII. COMPONENT VALUE DEVIATION

This section analyzes the effect of the resistor and capacitor value deviation. In a typical PPF the resistors and capacitors are in close proximity and the mismatch among resistor and capacitor values is usually well controlled in most IC processes. Therefore, the component mismatch is neglected in this analysis and only the minimum and maximum component deviations are considered. The effect of component mismatch is analyzed in [7] and [8], for example.

The relative maximum (ΔR_{max}) and minimum (ΔR_{min}) resistor value deviation from the typical value (R_{typ}) are defined in the following way:

$$\Delta R_{max} = \frac{R_{max} - R_{typ}}{R_{typ}} \rightarrow R_{max} = R_{typ} (1 + \Delta R_{max}), \quad (82)$$

$$\Delta R_{min} = \frac{R_{typ} - R_{min}}{R_{typ}} \rightarrow R_{min} = R_{typ} (1 - \Delta R_{min}). \quad (83)$$

The capacitor deviation is defined in a similar manner. Typically, the component deviation is symmetrical, i.e.

$$\Delta R_{max} \approx \Delta R_{min} = \Delta R. \quad (84)$$

Therefore, the resistor R_n of the n^{th} PPF stage could be replaced with $R_n \rightarrow R_n(1 \pm \Delta R_n)$ in all presented equations. The same can be done for the capacitors, too, $C_n \rightarrow C_n(1 \pm \Delta C_n)$. Clearly, the pole frequencies shift due to the device value variation.

$$\frac{1}{R_n C_n} \rightarrow \frac{1}{R_n (1 \pm \Delta R_n) C_n (1 \pm \Delta C_n)}. \quad (85)$$

It is possible that the pole frequency remains unchanged, because resistor and capacitor variations do not track each other. In the worst case, both the capacitor and resistor values vary in the same direction, i.e. only '+' or '-' signs apply. However, the pole splitting factor remains nearly unchanged, if the relative deviation is independent of the original component value. That holds, when all the devices are made of the same material and have similar geometry. For example, in a case of

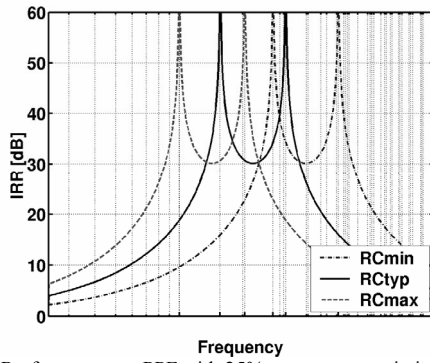


Fig. 20. IRR of a two-stage PPF with 25% component variation.

two stage-PPF, if $\Delta R_1 \cong \Delta R_2$ and $\Delta C_1 \cong \Delta C_2$, the pole splitting factor k_2 is

$$k_2 = \frac{R_2 C_2}{R_1 C_1} \rightarrow \frac{R_2 (1 \pm \Delta R_2)}{R_1 (1 \pm \Delta R_1)} \frac{C_2 (1 \pm \Delta C_2)}{C_1 (1 \pm \Delta C_1)} \approx k_2. \quad (86)$$

The unchanged pole splitting factor holds for the higher order PPFs, too. As a result, overall IRR remains unchanged but it shifts in the frequency domain. To achieve the required IRR over the whole wanted bandwidth and taking into account the device variation, the relative frequency BW_{rel} , defined as $\omega_{max}/\omega_{min}$, as in (25), (33), and (43), should be multiplied by bandwidth deviation factor (BW_{dev}) defined as:

$$BW_{dev} = \frac{R_{max} C_{max}}{R_{min} C_{min}} = \frac{(1 + \Delta R_{max})(1 + \Delta C_{max})}{(1 - \Delta R_{min})(1 - \Delta C_{min})}. \quad (87)$$

Therefore, the efficient relative factor $BW_{rel,eff}$ is defined:

$$BW_{rel,eff} = BW_{rel} BW_{dev}. \quad (88)$$

For example, a typical 25% ΔR and ΔC variation leads to $BW_{dev} = 2.78$. Therefore, the required relative bandwidth BW_{rel} nearly triples.

A. Geometric Center Frequency Deviation

When the PPF minimum (ω_{min}) and maximum (ω_{max}) operational frequencies are known, the geometric center frequency ω_c can be calculated as

$$\omega_c = \sqrt{\omega_{min} \omega_{max}} = \sqrt{BW_{rel}} \omega_{min} = \frac{\omega_{max}}{\sqrt{BW_{rel}}}. \quad (89)$$

The center frequencies of 1-, 2-, and 3-stage PPFs are $\omega_{c,1-stg} = \omega_1$, $\omega_{c,2-stg} = \omega_1/\sqrt{k_2}$, and $\omega_{c,3-stg} = \omega_1/k_2 = \omega_2$, respectively.

IRR performance of a 2-stage PPF ($k_2=2$) with minimum (RC_{min}), typical (RC_{typ}), and maximum (RC_{max}) component values ($\Delta R = \Delta C = 0.25$) are plotted in Fig. 20. The frequency, where IRRs with minimum and maximum deviations overlap, slightly differs from the geometric center frequency of a PPF with typical values. In a general case, the relative center frequency deviation can be calculated as

$$\Delta \omega_{RCdev} = \frac{\omega_{c,RCtyp}}{\omega_{c,RCdev}}. \quad (90)$$

In (90) $\omega_{c,RCtyp}$ is the geometric center frequency of the PPF with typical component values, $\omega_{c,RCdev}$ is the geometric center

frequency due to device variations, and thus $\Delta \omega_{RCdev}$ becomes

$$\begin{aligned} \Delta \omega_{RCdev} &= \sqrt{(1 - \Delta R_{min})(1 + \Delta R_{max})(1 - \Delta C_{min})(1 + \Delta C_{max})} \\ &\approx \sqrt{(1 - \Delta R^2)(1 - \Delta C^2)}. \end{aligned} \quad (91)$$

The last form of (91) holds when device value deviation is symmetrical according to (84). For example, with 25 % device variation, $\Delta \omega_{RCdev}$ is approximately 0.94. All the original pole frequencies ω_n of PPF with nominal device values should be multiplied by a factor $\Delta \omega_{RCdev}$ to achieve the required IRR over the whole wanted bandwidth and taking into account the device variation.

VIII. SUMMARY AND DESIGN EXAMPLE

In this section we summarize the results and provide a design example to clarify the design procedure. Below is a list of major design principles of an optimum PPF. Reasoning for each item is given in the analysis, and for sake of brevity, is not repeated here. A well-designed multi-stage PPF obeys the following rules:

- RC poles are split.
- Optimal pole splitting is calculated according to $BW_{rel,eff}$.
- The capacitors are of equal value in each stage.
- The impedance level (i.e. resistor values) increase along the signal chain.
- Component value deviation is taken into account, when the effective relative bandwidth $BW_{rel,eff}$ is calculated.
- The resistor values are calculated taking into account the termination impedances.
- Parasitic capacitance is kept equal in each node of a PPF stage.

For the design example given next, we have 40-dB IRR requirement, the wanted relative bandwidth BW_{rel} is 1.5, and component deviation $\Delta R = \Delta C = 0.25$. The source impedance (Z_S) is 100 Ω differentially and the load (Z_L) is a buffer with differential input impedance of 2 k Ω . The maximum corner frequency $\omega_{c,max}$ is scaled to 1. Then, the minimum corner frequency $\omega_{c,min} = 0.666$.

The design of a PPF starts by checking the needed number of stages. That depends on the IRR requirement and device value variation.

1. *Effective Relative Bandwidth*: According to (87), the bandwidth deviation BW_{dev} is 2.78. Therefore, the effective required bandwidth (88) becomes 4.17.
2. *Equal RC Poles*: According to (26), when $BW_{rel,eff} = 4.17$, the n -stage PPF with equal RC poles offers approximately $n \cdot 9.31$ -dB IRR performance. Therefore, a 5-stage PPF would be needed.
3. *Unequal RC Poles*: According to (32), in a two-stage PPF $k_2 = 2.69$ is needed to fulfill $BW_{rel,eff}$ requirement leading to less than 25-dB IRR (29). When 3-stage PPF is utilized instead, with (43) k_2 can be solved to be 1.838. (39) gives IRR of 40.2 dB, which is adequate. The requirement for number of stages could be quickly checked from Fig. 9.

CAS-I 5126 Kaukovouri

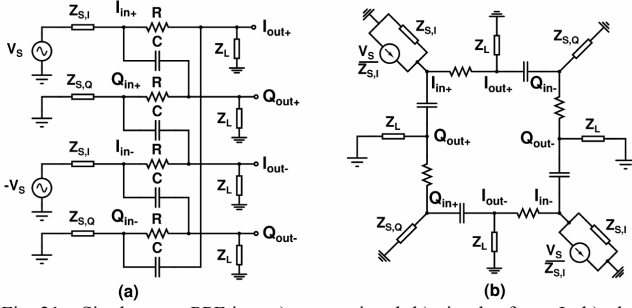


Fig. 21. Single-stage PPF in a) conventional, b) circular form. In b), the voltage source is replaced with Norton equivalent.

When the number of PPF stages is known, the pole frequencies are calculated. The effect of component deviation is also taken into account. The design values are given for a 3-stage PPF. In addition, the references to equations to evaluate corresponding design values for a 2-stage PPF are given in parenthesis.

4. *Pole Frequencies*: The geometric center frequency ω_2 can be calculated with (89), $\omega_2 \approx 0.816$. The other poles, ω_1 and ω_3 , are achieved with (28), (35), and (38): $\omega_1 \approx 1.501$, $\omega_3 \approx 0.444$. (2-stage PPF: (89), (28))
5. *Pole Shifting*: The device value deviation causes the geometric center frequency deviation. According to (91), the relative center frequency shift factor $\Delta\omega_{RCdev} = 0.9375$. Therefore, all the pole frequencies are shifted to lower frequencies by that factor. The final pole frequencies are therefore $\omega_1 \approx 1.407$, $\omega_2 \approx 0.765$, and $\omega_3 \approx 0.416$.

When termination impedances are known, the optimal device value can be calculated. In addition, the choice of PPF type is done.

6. *Optimal Device Values*: Based on termination impedance relation (60) $k_2 = 20$. The capacitor values are assumed to have only one value through the whole PPF, and therefore pole splitting is done by scaling the resistor values only. The optimum k_L -values are given by (69) and (70), and they are $k_{L,opt}^I = 9.714$ and $k_{L,opt}^{II} = 6.869$ for Type I and Type II PPFs, respectively. Therefore, the R_I values calculated with (59) are 233Ω and 330Ω for Type I and Type II PPFs, respectively. The other resistor values are calculated with (28) and (35), i.e. R_2 and R_3 are 429Ω and

788Ω for Type I PPF, and 606Ω and 1115Ω for Type II PPF, respectively. The capacitor values are finally dimensioned with the pole frequencies defined in Step 5. $C_1 = C_2 = C_3 = 1/\omega_j R_I$ i.e. 3.05 mF and 2.15 mF for Type I and Type II, respectively. (2-stage PPF: (60), (67), (68), (59), (28))

7. *Loss*: The loss without the effect of parasitics can be checked from Fig. 16. When $k_2 = 20$ and $k_2 \approx 1.838$, the overall loss of Type I and Type II PPFs are approximately 10 dB and 8.4 dB, respectively. Therefore, it is optimal to choose Type II PPF to minimize the LO signal loss if the system allows frequency deviation of 1.15° .
8. *The Effect of Parasitics*: With modern IC processes, the bottom plate capacitance of capacitors is rather small, less than 10%. According to Fig. 19, the additional loss at ω_1 is approximately 2 dB with three-stage PPF with k_2 of 1.838 regardless of PPF type.

APPENDIX A: PROOF OF VIRTUAL GROUND

In this appendix is proven, that when I-inputs are excited with a balanced signal then Q-inputs are virtual grounds. This also applies vice versa, i.e. when Q-inputs are excited with a balanced signal then I-inputs are virtual grounds. A single polyphase filter stage is shown in Fig. 21. The input impedances of I-input and Q-inputs are $Z_{s,I}$ and $Z_{s,Q}$, respectively. Different input impedances for I and Q-inputs are utilized to show that the virtual grounds at Q-inputs do not depend on $Z_{s,I}$ and virtual grounds exist whatever the $Z_{s,Q}$ is. The load impedance is Z_L . For the convenience, the PPF also is redrawn into a circular form and the signal source V_s is formed to a Norton equivalent.

The Proof.

The PPF is analyzed with a nodal method, i.e. by solving the equation $\mathbf{Y} \cdot \mathbf{V} = \mathbf{I}$, where admittance matrix \mathbf{Y} presents the circuit, the voltage vector \mathbf{V} includes the voltages associated to each node, and the current vector \mathbf{I} includes the currents at each node. \mathbf{Y} , \mathbf{V} , and \mathbf{I} for a PPF stage shown in Fig. 21b are given in (A.1). The voltage at node I_{in+} is marked with $V_{I_{in+}}$

$$\begin{bmatrix} 1/Z_{s,I} + sC + 1/R & -sC & 0 & 0 & 0 & 0 & 0 & -1/R \\ -sC & 1/Z_L + sC + 1/R & -1/R & 0 & 0 & 0 & 0 & 0 \\ 0 & -1/R & 1/Z_{s,Q} + sC + 1/R & -sC & 0 & 0 & 0 & 0 \\ 0 & 0 & -sC & 1/Z_L + sC + 1/R & -1/R & 0 & 0 & 0 \\ 0 & 0 & 0 & -1/R & 1/Z_{s,I} + sC + 1/R & -sC & 0 & 0 \\ 0 & 0 & 0 & 0 & -sC & 1/Z_L + sC + 1/R & -1/R & 0 \\ 0 & 0 & 0 & 0 & 0 & -1/R & 1/Z_{s,Q} + sC + 1/R & -sC \\ -1/R & 0 & 0 & 0 & 0 & 0 & -sC & 1/Z_L + sC + 1/R \end{bmatrix} \begin{bmatrix} V_{I_{in+}} \\ V_{Q_{out+}} \\ V_{Q_{in+}} \\ V_{I_{out-}} \\ V_{I_{in-}} \\ V_{Q_{out-}} \\ V_{Q_{in-}} \\ V_{I_{out+}} \end{bmatrix} = \begin{bmatrix} V_s / Z_{s,I} \\ 0 \\ 0 \\ 0 \\ -V_s / Z_{s,I} \\ 0 \\ 0 \\ 0 \end{bmatrix} \quad (\text{A.1})$$

$$\mathbf{Y}^* = \begin{bmatrix} 1/Z_{s,I} + sC + 1/R & -sC & V_s / Z_{s,I} & 0 & 0 & 0 & 0 & -1/R \\ -sC & 1/Z_L + sC + 1/R & 0 & 0 & 0 & 0 & 0 & 0 \\ 0 & -1/R & 0 & -sC & 0 & 0 & 0 & 0 \\ 0 & 0 & 0 & 1/Z_L + sC + 1/R & -1/R & 0 & 0 & 0 \\ 0 & 0 & -V_s / Z_{s,I} & -1/R & 1/Z_{s,I} + sC + 1/R & -sC & 0 & 0 \\ 0 & 0 & 0 & 0 & -sC & 1/Z_L + sC + 1/R & -1/R & 0 \\ 0 & 0 & 0 & 0 & 0 & -1/R & 1/Z_{s,Q} + sC + 1/R & -sC \\ -1/R & 0 & 0 & 0 & 0 & 0 & -sC & 1/Z_L + sC + 1/R \end{bmatrix} \quad (\text{A.2})$$

etc. For example, when the voltage at node Q_{in+} is being solved, the third column of admittance matrix \mathbf{Y} is replaced with the current source vector \mathbf{I} . The resulting matrix is \mathbf{Y}^* , see (A.2). Next, $V_{Q_{in+}}$ is solved by calculating the determinants of the matrices \mathbf{Y} and \mathbf{Y}^* and dividing them:

$$V_{Q_{in+}} = \frac{\text{Det}[\mathbf{Y}^*]}{\text{Det}[\mathbf{Y}]} \quad (\text{A.3})$$

Since the numerator equals to zero, the node Q_{in+} is a virtual ground. The same could be repeated for Q_{in-} , as well. Since nodes Q_{in+} and Q_{in-} are virtual grounds, equivalent load shown in Fig. 3 (b) results. To prevent division by zero, i.e. $\text{Det}[\mathbf{Y}] \neq 0$, $\Re(Z_{S,I}) > 0$, $\Re(Z_{S,Q}) > 0$, $R > 0$, and $\Re(Z_L) \geq 0$ are required, which in practice is so.

APPENDIX B: ANALYSIS AND OPTIMIZATION OF 4-STAGE PPF

The optimum pole splitting is calculated for a four-stage PPF. First, the pole splitting factor k_4 is defined as the ratio of the pole frequencies ω_l and ω_4 . Due to symmetry reasons, the pole ratio between ω_3 and ω_4 is the same as the pole ratio between ω_l and ω_2 . Thus, k_4 is determined by k_2 and k_3

$$k_4 = \frac{\omega_l}{\omega_4} = \frac{\omega_l}{\omega_3} \frac{\omega_3}{\omega_4} = k_3 k_2 \quad (\text{B.1})$$

The minimum IRRs are achieved at three frequencies given by

$$\omega_{IRR, \min 2} = \frac{\omega_1}{\sqrt{k_2 k_3}} \quad (\text{B.2})$$

$$\omega_{IRR, \min 1,3} = \frac{\omega_1}{\sqrt{2k_2 k_3}} \sqrt{F_3(k_2, k_3) \pm \sqrt{F_3(k_2, k_3)^2 - 4k_2^2 k_3^2}} \quad (\text{B.3})$$

where

$$F_3(k_2, k_3) = k_2(1-k_3)^2 + k_3(1-k_2)^2 + 2k_2 k_3 \quad (\text{B.4})$$

The IRR minimums at $\omega_{IRR, \min 1}$ and $\omega_{IRR, \min 3}$ are always equal. To achieve equal IRR with $\omega_{IRR, \min 2}$, too, k_3 is calculated as

$$k_3 = \frac{1}{3k_2} \left[k_2(k_2^2 + k_2 - 1) + F_4(k_2) \cos \left(\frac{1}{3} \arccos \left(\frac{F_5(k_2)}{F_4(k_2)^3} \right) \right) \right] \quad (\text{B.5})$$

where

$$F_4(k_2) = 2\sqrt{k_2(k_2^5 + 2k_2^4 - k_2^3 - 5k_2^2 + 4k_2 + 3)} \quad (\text{B.6})$$

$$F_5(k_2) = 4k_2^2 \left(-9 + k_2 \left(-9k_2^3 + 2(-1 + k_2 + k_2^2)^3 \right) \right) \quad (\text{B.7})$$

Equation (B.5) is quite tedious for hand calculations. Therefore, an approximate formula for k_3 calculation given as

$$k_3 \approx 1.2k_2^2 + 0.17k_2 - 0.37 \quad (\text{B.8})$$

will predict (B.5) with an maximum error of 1.1% when $k_2 < 3$. At $\omega_{IRR, \min 2}$ the amplitude balance becomes

$$A_{bal, 4\text{-stg}} = \frac{k_2(1+k_3)^2 + k_3(1+k_2)^2}{2\sqrt{k_2 k_3}(k_2+1)(k_3+1)} \quad (\text{B.9})$$

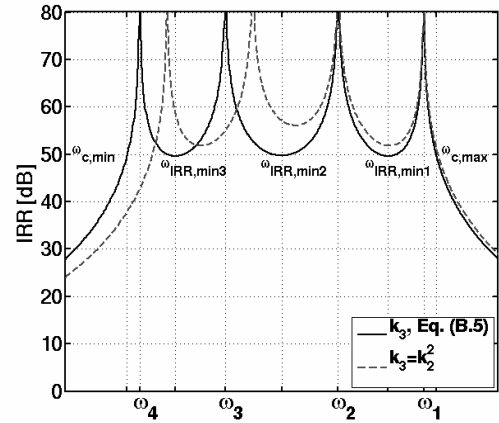


Fig. 22. IRR of a 4th order PPF. With a solid line, a BW optimized PPF is shown. In that case, k_3 is calculated with (B.5). With a dashed line, k_3 is calculated as k_2^2 . In both cases, $k_2 = 1.6$.

from where the IRR can be calculated with (19). The corner frequencies $\omega_{c, \min}$ and $\omega_{c, \max}$, where the minimum IRR is achieved, can be calculated with

$$\omega_{c, \min \& \max} = \frac{\omega_l}{(4k_2 k_3)^{3/2}} \left(F_6^+(k_2, k_3) + F_6^-(k_2, k_3) \pm 2\sqrt{F_6^+(k_2, k_3)F_6^-(k_2, k_3)} \right) \quad (\text{B.10})$$

where the '+' or '-' sign of F_6 is chosen according to

$$F_6^\pm(k_2, k_3) = k_2(k_3 \pm 1)^2 + k_3(k_2 \pm 1)^2 \quad (\text{B.11})$$

The relative bandwidth, where the IRR_{\min} is achieved, is

$$BW_{rel, 4\text{-stg}} = \frac{F_6^+(k_2, k_3) + F_6^-(k_2, k_3) + 2\sqrt{F_6^+(k_2, k_3)F_6^-(k_2, k_3)}}{F_6^+(k_2, k_3) + F_6^-(k_2, k_3) - 2\sqrt{F_6^+(k_2, k_3)F_6^-(k_2, k_3)}} \quad (\text{B.12})$$

Equation (B.12) can be approximated with better than 1.0-% accuracy with

$$BW_{rel, 4\text{-stg}} \approx 2.73k_2^3 - 3.63k_2^2 + 2.9k_2 - 1, \quad (\text{B.13})$$

when $k_2 < 3$. The minimum IRR and relative bandwidth with optimum pole splitting are shown in Fig. 8.

If the IRR is calculated for a 4-stage PPF by using (B.5), quite complicated equations are achieved. To get a simple equation for 4th-order PPF IRR, the generic formula $k_{n+1}/k_n = k_2$ is used to calculate pole splitting factors k_3 and k_4 . As a result, the IRR at the frequency given by (B.2) becomes

$$IRR_{\min, 4\text{-stg}} = \left(\frac{\sqrt{k_2} + 1}{\sqrt{k_2} - 1} \right)^4 \left(\frac{k_2 - \sqrt{k_2} + 1}{k_2 + \sqrt{k_2} + 1} \right)^2 \quad (\text{B.14})$$

Compared to other two IRR minimums at frequencies given by (B.3), IRR of (B.14) is approximately 5 dB higher when k_2 is close to unity. This is shown in Fig. 22, where the IRR of a 4th order PPF is shown. With a solid line, a BW-optimized PPF is shown. In that case, k_3 is calculated with (B.5). With a dashed line, k_3 is calculated as k_2^2 . In both cases $k_2 = 1.6$ and k_4 is calculated as in (B.1).

REFERENCES

- [1] B. Razavi, *RF microelectronics*. Prentice-Hall, 1998, p. 335.

CAS-I 5126 Kaukovuori

- [2] A. A. Abidi, "Direct-conversion radio receivers for digital communications," *IEEE J. Solid-State Circuits*, vol. 30, pp. 1399-1410, no. 12, Dec. 1995.
- [3] J. Crols, M. S. J. Steyaert, "A single-chip 900 MHz CMOS receiver front-end with a high performance low-IF topology," *IEEE J. Solid-State Circuits*, vol. 30, pp. 1483-1492, no. 12, Dec. 1995.
- [4] A. Y. Valero-Lopez, S. T. Moon, E. Sánchez-Sinencio, "Self-calibrated quadrature generator for WLAN multistandard frequency synthesizer," *IEEE J. Solid-State Circuits*, vol. 41, pp. 1031-1041, no. 5, May 2006.
- [5] M. J. Gingell, "Single sideband modulation using sequence asymmetric polyphase networks," *Electrical Communication*, vol. 48, pp. 21-25, no. 1 and 2, 1973.
- [6] R. C. V. Macario and I. D. Mejjallie, "The phasing method for sideband selection in broadcast receivers," *EBU Review (Technical Part)*, no. 181, pp. 119-125, 1980.
- [7] S. H. Galal, H. F. Ragaie, and M. S. Tawfik, "RC sequence asymmetric polyphase filters for RF integrated transceivers," *IEEE Trans. on Circuits and Systems—II: Analog and Digital Signal Processing*, vol. 47, pp. 18-27, no. 1, Jan. 2000.
- [8] F. Behbahani, Y. Kishigami, J. Leete, and A. A. Abidi, "CMOS mixers and polyphase filters for large image rejection," *IEEE J. Solid-State Circuits*, vol. 36, pp. 873-887, no. 6, June 2001.
- [9] K. Wada and Y. Tadokoro, "RC polyphase filter with flat gain characteristic," *In Proc. IEEE Int. Symp. On Circuits and Systems (ISCAS) 2003*, Bangkok, Thailand, May 25-28, 2003, pp. I-537-I-540.
- [10] H. Kobayashi, T. Kitahara, S. Takigami, and H. Sadamura, "Explicit transfer function of RC polyphase filter for wireless transceiver analog front-end," *In Proc. 2002 IEEE Asia-Pacific Conference on ASIC (AP-ASIC 2002)*, Taipei, Taiwan, Aug. 6-8, 2002, pp. 137-140.
- [11] N. Yamaguchi, H. Kobayashi, J. Kang, Y. Niki, and T. Kitahara, "Analysis of RC polyphase filters – high-order filter transfer functions, Nyquist charts, and parasitic capacitance effects," *IEICE Technical Meeting of Circuits and Systems*, Wakayama, Japan, p. 6, Jan. 2003.
- [12] Y. Niki, J. Kang, H. Kobayashi, N. Yamaguchi, and T. Kitahara, "Analysis of RC polyphase filters – input impedance, output termination, component mismatch effects, flat-passband filter design," *IEICE Tech. Meeting of Circuits and Systems*, Wakayama, Japan, p. 6, Jan. 2003.
- [13] J. W. Archer, J. Granlund, and R. E. Mauzy, "A broad-band UHF mixer exhibiting high image rejection over a multidecade baseband frequency range," *IEEE J. Solid-State Circuits*, vol. SC-16, pp. 385-392, no. 4, Aug. 1981.
- [14] E. Tiiliharju and K. Halonen, "A broadband quadrature-modulator in standard 0.13 μm CMOS," *Analog Integrated Circuits and Signal Processing*, vol. 46, pp. 37-46, no. 1, Jan. 2006.
- [15] W. B. Mikhael, "Sequence discriminators and their use in frequency division multiplex-communication systems," *IEEE Trans. on Circuits and Systems*, vol. CAS-26, pp. 117-129, no. 2, Feb. 1979.
- [16] D. E. Norgaard, "The phase-shift method of single-sideband signal reception," *Proceedings of the IRE*, vol. 44, pp. 1735-1743, Dec. 1956.



Jussi Rynnänen (S'99-M'04) was born in Ilmajoki, Finland, in 1973. He received the Master of Science, Licentiate of Science, and Doctor of Science degrees in electrical engineering from the Helsinki University of Technology (HUT), Helsinki, Finland, in 1998, 2001, and 2004, respectively. He is currently working as a full professor in Electronic Circuit Design Laboratory. His main research interests are RF circuits, low-noise amplifiers and mixers in direct-conversion receivers.



Kari A. I. Halonen (M'02) received the M.Sc. degree in electrical engineering from Helsinki University of Technology, Finland, in 1982, and the Ph.D. degree in electrical engineering from the Katholieke Universiteit Leuven, Belgium, in 1987. Since 1988 he has been with the Electronic Circuit Design Laboratory, Helsinki University of Technology. From 1993 he has been an associate professor, and since 1997 a full professor at the Faculty of Electrical Engineering and Telecommunications. He became the Head of Electronic Circuit Design Laboratory year 1998. He has been an associate editor of IEEE Transactions on Circuits and Systems I, a guest editor for IEEE Journal of Solid-State Circuits and the Technical Program Committee Chairman for European Solid-State Circuits Conference year 2000. He has been awarded the Beatrice Winner Award in ISSCC'02 Conference year 2002. He is a TPC-member of ESSCIRC and ISSCC. He specializes in CMOS and BiCMOS analog integrated circuits, particularly for telecommunication applications. He is author or co-author over two hundred international and national conference and journal publications on analog integrated circuits.



Jouni Kaukovuori (S'05) was born in 1977. He received the M.Sc. degree in electrical engineering from the Helsinki University of Technology (HUT), Helsinki, Finland, in 2002. He is currently working toward the D.Sc. degree at the same university. From 2001 to 2007, he was a Research Engineer with Electronic Circuit Design Laboratory at HUT. Since June 2007, he has been with Nokia Corp., Helsinki, where he is currently a Research Specialist. His main research interests are CMOS RF circuits for wireless

applications.



Kari Stadius (S'95-M'03) received the M.Sc degree in electrical engineering in 1994 and the Licentiate of Technology degree in 1997, both from Helsinki University of Technology, where he is currently working as a research scientist. His research interests include the design and analysis of RF transceiver blocks with special emphasis on frequency synthesizers, RF oscillators and modeling of passive components.